Global and Planetary Change 259 (2026) 105327

Contents lists available at ScienceDirect

Global and Planetary Change

journal homepage: www.elsevier.com/locate/gloplacha

Persistence and resilience on Mount Etna's active flank: An integrated geological and archaeological perspective

Carla Bottari [a,*], Alessandro Luppino [b], Salvatore Claudio Alparone [a], Francesca Forni [c], Gianluca Groppelli [d], Mimmo Palano [e,a], Francesco Sortino [f], Salvatore Giammanco [a]

[a] Istituto Nazionale di Geofisica e Vulcanologia, Sezione Osservatorio Etneo, 95125 Catania, Italy
[b] Dipartimento di Scienze dell'Ambiente e della Terra (DISAT), Università degli Studi di Milano Bicocca, 20126 Milano, Italy
[c] Dipartimento di Scienze della Terra "Ardito Desio", Università degli Studi di Milano Statale, 20133 Milano, Italy
[d] Consiglio Nazionale delle Ricerche (CNR), Istituto di Geologia Ambientale e Geoingegneria (IGAG), 20131 Milano, Italy
[e] Dipartimento di Scienze della Terra e del Mare, Università degli Studi di Palermo, 90123 Palermo, Italy
[f] Istituto Nazionale di Geofisica e Vulcanologia, Sezione Palermo, 90146 Palermo, Italy

ARTICLE INFO

Editor: Dr. Sun Jimin

Keywords:
Mount Etna
Volcanic and seismic hazards
Human resilience
Hydrothermal systems
Flank instability
Archaeoseismology
Geological–archaeological integration

ABSTRACT

Volcanic environments illustrate how human communities have learned to persist within dynamic, hazardous landscapes by balancing risk and opportunity. Mount Etna (Sicily, Italy) – one of the world's most active volcanoes – provides an outstanding natural laboratory to investigate the interplay between geodynamic and volcanic processes as well as human adaptation. The site of Santa Venera al Pozzo (SVP) exemplifies this duality: archaeological and geological evidence reveal a persistent human presence since the Late Neolithic, sustained by fault-controlled hydrothermal discharge and a geomorphological position that ensured long-term stability outside major lava flow pathways.

This study integrates geological, geochemical, geodetic, seismological, and archaeological data to examine how tectonic and magmatic processes sustained hydrothermal activity and supported enduring settlement. Results indicate that (i) deformation was largely accommodated by creeping faults, in turn enhancing permeability and maintaining spring discharge; (ii) the site's distal position from eruptive rift zones provided geomorphological stability; and (iii) cultural practices promoted the adaptive reuse of geothermal resources over the time.

The case of SVP demonstrates that the same Earth processes generating hazards also maintain vital resources, enabling long-term human resilience. This integrated geological–archaeological perspective provides a transferable framework for understanding sustainability and risk in volcanically active regions worldwide.

1. Introduction

For millennia, human populations have persisted in volcanic environments, attracted by fertile soils, abundant water, and stable hydrothermal resources, despite the inherent risks (James et al., 2000; Small and Naumann, 2001; Barclay et al., 2019; Vergara-Pinto and Marín, 2023). Volcanic soils, enriched with minerals from weathering of the eruptive products (lavas and tephra), support fertile agriculture, and their high permeability enhances groundwater storage and distribution (Berger, 2006). However, these benefits are accompanied by multiple hazards, including seismic activity, lava flows and pyroclastic density current invasion, as well as toxic gas emissions.

Recent perspectives from social volcanology emphasize that human settlement near volcanoes reflects not only environmental opportunity but also cultural adaptation and risk negotiation (Kelman and Mather, 2008; Prayoga et al., 2024). Communities have historically developed technological, spatial, and symbolic strategies to coexist with instability, transforming volcanic landscapes into resilient socio-ecological systems (Torrence, 2019; Riede et al., 2020).

Mount Etna volcano located on the eastern coast of Sicily (Italy) at the convergent margin between the African and Eurasian plate (Gvirtzman and Nur, 1999), exemplifies the dual nature of opportunity and risk. Its frequent eruptions have continuously reshaped the landscape and disrupted local communities. Nonetheless, archaeological evidence suggests persistent human presence along its flanks since the Late Neolithic, through Greek, Roman, and Medieval periods (2021;

* Corresponding author.
E-mail address: carla.bottari@ingv.it (C. Bottari).

https://doi.org/10.1016/j.gloplacha.2026.105327
Received 2 September 2025; Received in revised form 20 January 2026; Accepted 20 January 2026
Available online 26 January 2026

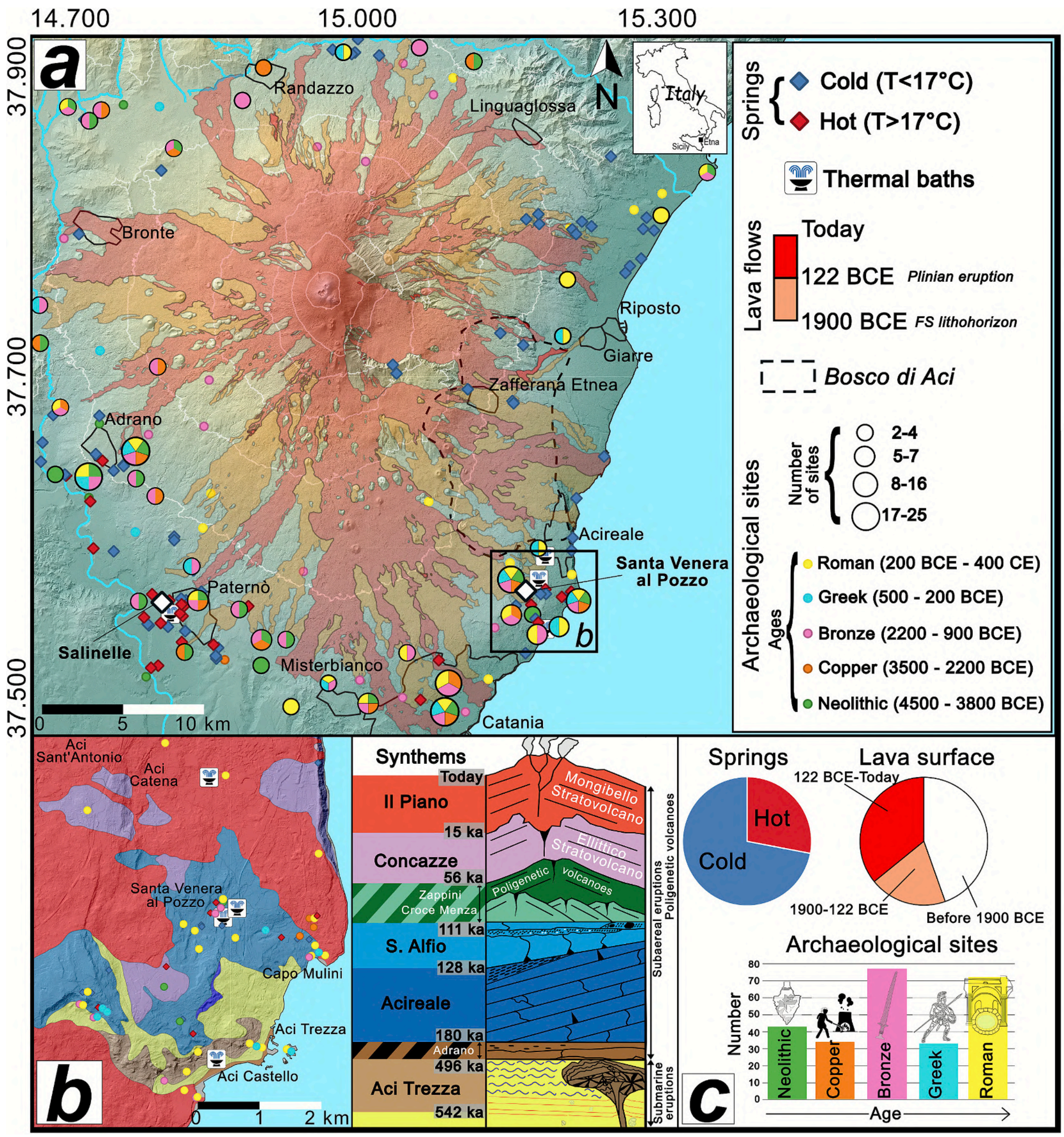

Fig. 1. Map of Mount Etna showing the location of key archaeological sites and geothermal features. (a) Historical and pre-historical lava flows on Mount Etna with major archaeological sites and thermal springs. Santa Venera al Pozzo and the Salinelle of Paternò are highlighted, together with cold springs and historical thermal baths. Archaeological sites are scaled according to the number of preserved structures and colour-coded by cultural period (Biscari, 1781; Brancato and Tortorici, 2021; Branca et al., 2021). Lava flows from Branca et al. (2011) and Proietti et al. (2024). Springs and related temperatures from Brusca et al., (2001). (b) Close-up of the SVP area showing archaeological features and hydrothermal manifestations (Brusca et al., 2001), superimposed on synthems (Branca et al., 2011; De Beni et al., 2011): Aci Trezza (pillow lavas from submarine eruptions on a sedimentary basement), Acireale (massive lava flows from fissural subaerial eruptions), S. Alfio (lavas and pyroclastics from subaerial eruptions), Concazze and Il Piano (lavas and pyroclastics from polygenetic volcanoes). Synthems indicated with colored patterns are outside the study area and not discussed. (c) Pie charts showing the proportions of hot and cold springs, and a histogram illustrating the distribution of archeological sites by age.

Brancato and Tortorici, 2021; Branca et al., 2021; Fig. 1).

The Acireale Plain on the southeastern flank has historically represented an important center for trade, agriculture, and cultural exchange. Comparable settlements such as Paternò and Adrano also developed along Mount Etna's lower slopes, where fertile volcanic soils and spring-fed water sources sustained agricultural activities. However, unlike these sites—often affected by lava flows, seismic damage, or periodic abandonment (Branca and Del Carlo, 2004)—Santa Venera al Pozzo (SVP) maintained a more continuous occupation through time and represents one of the earliest settlements on the southeastern flank of Mount Etna, with origins dating back to 3000–2200 BCE (Brancato and Tortorici, 2021; Branca et al., 2021). Among the various settlements in this area, SVP stands out for its remarkable longevity, sustained by the presence of thermal springs, its location near the ancient port of Capo Mulini, the natural barrier provided by the Bosco delle Aci—which shows no archaeological evidence of settlement (Sartorius von Waltershausen, 1859)—and its strategic position along the Roman Pompeian road (Calderone and De Giorgi, 2024; Fig. 1a). At present, SVP is not permanently inhabited; the archaeological area alone preserves evidence of long-term human activity, confirming that settlement persistence is documented exclusively through the archaeological record rather than modern occupation.

In addition to water and soil resources, the area includes clay-rich deposits exploited since prehistoric times for ceramic and construction materials (Calderone and De Giorgi, 2024). These deposits, mapped in the SVP area (Fig. 1b), consist of alternating lava flows and volcaniclastic layers with sedimentary intercalations that contribute to the heterogeneity of the near-surface substrate. Moreover, fault systems related to Mount Etna's complex volcano-tectonic framework have significantly influenced the local topography (Fig. 2). Particularly,

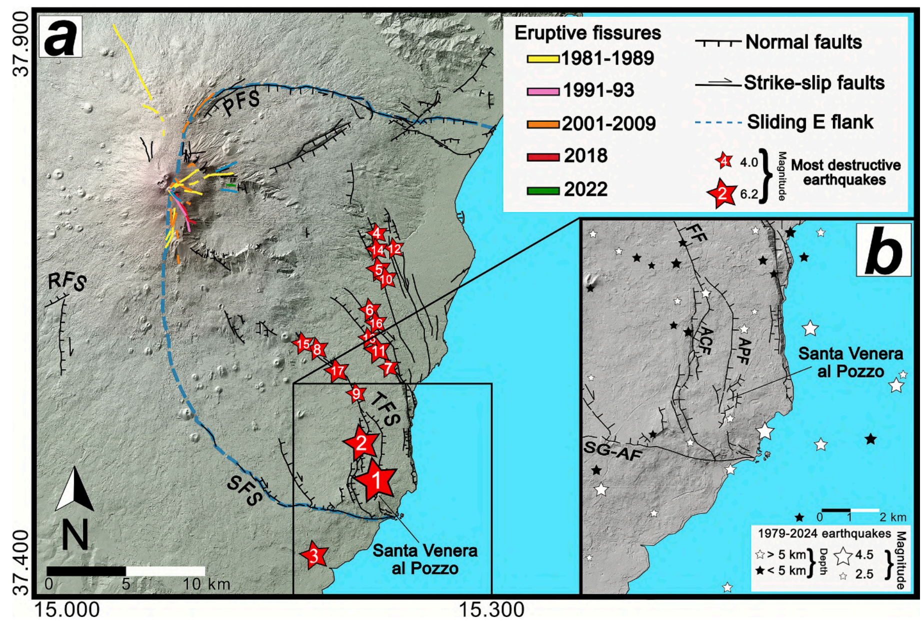

Fig. 2. Volcano-tectonic structures and seismicity of Mount Etna's southeastern flank. (a) Main fault systems and eruptive fissures. Fault abbreviations: PFS = Pernicana Fault System; RFS = Ragalna Fault System; SFS = South Fault System; TFS = Timpe Fault System; FF = Fiandaca Fault; SG–AF = San Gregorio–Acitrezza Fault; APF = Aci Platani Fault; ACF = Aci Catena Fault. Epicenters of major historical earthquakes are shown as stars and numbered according to their reference in Table 1 (Guidoboni et al., 2014, 2019; Azzaro and D'Amico, 2019). (b) Instrumental seismicity from 1981 to 2024, colour-coded by depth. Faults data from Branca et al. (2011) and Azzaro et al. (2012); eruptive fissures from Bevilacqua et al. (2022) and Proietti et al. (2024).

tectonic coastal uplift provided a natural protection from marine incursions and potential invasions, while active faults controlled the deep circulation of thermal fluids. These structures channel magmatic and meteoric waters to the surface, forming geothermal springs historically used for bathing, irrigation, and ritual activities (Liotta et al., 2017; Branca et al., 2021). Geochemical anomalies—including high CO_2 degassing and temporal variations in water composition—reflect the dynamic interaction between tectonics and magmatism (Sortino et al., 2022).

This review highlights the paradox of hazard and opportunity on Etna's southeastern flank, framing Santa Venera al Pozzo as a natural laboratory to explore how geodynamic and volcanic processes foster resilience in volcanic landscapes and how societies transform hazardous environments into sustainable habitats.

Despite decades of geological and archaeological research, some relevant key questions have remained unanswered:

- How do volcano-tectonic and magmatic processes influence hydrothermal fluid migration across Etna's southern flank, and how are these reflected in the archaeological record?
- What role did hydrothermal systems play in sustaining ancient settlements, and how did local communities mitigate geohazards through spatial, architectural, and symbolic strategies?

To address these questions, we combine geological, geochemical, geodetic, and seismological data with the archaeological record. Our aim is to explore how deep Earth processes and human responses co-evolved, producing a model of long-term resilience on Mount Etna. This framework may be transferable to other volcanically active regions worldwide.

2. Etna's unstable flank: volcanic activity, tectonics and gravitational dynamics

2.1. Eruptive dynamics and settlement exposure

Mount Etna's activity is predominantly effusive, characterized by frequent lava flows interrupted by occasional high-energy explosive phases, including rare Plinian-style eruptions, such as the 122 BCE event (Coltelli et al., 1998; Branca and Del Carlo, 2004). Over the past 15,000 years, Mount Etna has predominantly erupted low viscosity basaltic lavas, which have flowed extensively across its flanks, reshaping the landscape and covering approximately 85% of its pre-existing surface (Branca et al., 2011; Branca et al., 2015). Flank eruptions—more frequent than those from the summit—preferentially exploit structural weaknesses along NE, ENE, S, and W rift zones, posing major hazards to settlements, especially on the densely populated southeastern flank, where eruptive vents often open at low elevations (Tibaldi and Groppelli, 2002; Azzaro et al., 2012; Branca et al., 2017; Tibaldi et al., 2025). Although less common, explosive events can generate high-altitude ash columns and widespread pyroclastic fallout. At least six widespread tephra layers have been recognized as stratigraphic regional markers, while numerous local scoria fall deposits are preserved in the volcanic record (Branca and Del Carlo, 2004; Del Carlo et al., 2004; Branca et al., 2025).

In recent decades, summit activity has been dominated by short-lived but intense paroxysmal eruptions. Despite their low eruptive volume, these events can cause significant societal disruption through widespread ashfall, affecting downwind communities—including densely populated towns on the southeastern flank—and disrupting regional air traffic (Barsotti et al., 2010). This eruptive behavior highlights the volcano's dual nature—continuously reshaping the territory while sustaining long-term human presence. However, the SVP area appears to have remained unaffected by direct lava inundation over the past millennia (Fig. 1b). This inference is supported by its favorable geomorphological position on a gently sloping, distal sector of the southeastern flank, located far from the main rift zones and from the Valle del Bove collapse depression, which collectively channel most flank eruptions (Branca et al., 2011). As a result, SVP constitutes a localized zone of relative geomorphological stability, providing long-term protection within an otherwise highly active volcanic landscape and explaining the persistence of settlement in proximity to a major eruptive system.

2.2. Tectonic controls and gravitational sliding

Mount Etna's southeastern flank is affected by an interaction between volcanic activity, regional tectonics, and gravitational deformation. This sector represents one of the largest active volcanic landslides in the world, involving the slow seaward displacement of the eastern flank at rates up to 30–50 mm/yr (Borgia et al., 1992; Lundgren et al., 2003; Solaro et al., 2010; Ruch et al., 2012).

Etna's deformation field is governed by the interplay of three primary stress sources: (i) regional N—S compression along the Ionian margin, (ii) crustal overpressure induced by magma intrusion and storage, and (iii) long-term gravitational sliding of the volcano's eastern flank.

The N-S regional compression has been inferred by geological observations, in-situ stress measurements (Bousquet et al., 1988), and deep earthquake focal mechanisms (Cocina et al., 1998), reflecting the ongoing convergence between the African and Eurasian plates (Gvirtzman and Nur, 1999). Available GNSS data highlighted that such a convergence is currently occurring at a rate of about ~5–6 mm/yr (Palano et al., 2023).

Continuous magma recharge and shallow intrusions have also been documented by volcanological observations (Branca et al., 2011) and geophysical monitoring (Harris et al., 2011; Bonaccorso and Calvari, 2013; Palano et al., 2024). As previously inferred (Bonaccorso and Calvari, 2013; Palano et al., 2024), only a moderate fraction (~30%) of the recharging magma is erupted, while the remaining (~70%) accumulates within the shallower plumbing system, contributing to the endogenous growth of the intrusive complex and to the gravitational instability of the volcanic edifice. This combination of magmatic, tectonic, and gravitational forcing produces a complex deformation pattern expressed by fault creep, block tilting, and episodic slow slip events.

Satellite and ground-based geodetic data reveal that deformation is not uniformly distributed over the entire volcanic edifice, but mainly concentrates on its eastern flank along the Timpe fault system, a set of en échelon fault scarps extending between Aci Catena, Aci Trezza, and Santa Tecla (Azzaro et al., 2013; Solaro et al., 2010; Bonforte et al., 2019).

Field and remote-sensing observations of the 2002 and 2022 surface-rupture events further confirm the role of aseismic creep and gravitational sliding on the lower eastern flank (Tringali et al., 2023). These structures act as boundaries between zones of differential motion, accommodating both elastic strain accumulation and aseismic creep.

The long-term gravitational instability of the eastern sector has been widely observed since the 1990s through both GNSS and InSAR data (Palano et al., 2024 and references therein). In addition, episodic slow slip events (SSEs)—producing several centimeters of displacement over timescales of hours to weeks—have been detected along the volcano's unstable southeastern slope (Palano et al., 2022). This sector is also characterized by active fault systems that exhibit both seismic and aseismic (creeping) behavior. These include the N-S striking Timpe Fault System (TFS; Azzaro et al., 2013; Fig. 2a) and the *E*-W trending Southern Etna Shear Zone (Firetto Carlino et al., 2019). While the TFS accommodates part of flank motion, its offshore continuation remains uncertain. Specifically, where TFS reaches the Ionian coastline north of Catania, its connection to the offshore San Gregorio–Acitrezza Fault (SG-AF) is ambiguous as documented previously (Azzaro et al., 2013; Gross et al., 2016) (Fig. 2b). This uncertainty highlights the structural complexity of the region, shaped by the superposition of gravitational sliding, magmatic intrusions, and regional compression. As a result, the geometry and kinematics of the fault network remain only partially constrained, and their role in localizing surface deformation, controlling hydrothermal pathways, and modulating seismic hazard continues to be actively debated (Bousquet and Lanzafame, 2004; Neri et al., 2004; Apuani et al., 2013).

Table 1
Historical and instrumental earthquakes affecting the southeastern flank of Mount Etna. Chronological list of major seismic events with macroseismic intensity ($7 \leq I_0 \leq 10$, MCS scale), magnitude (M_m for historical events*; M_w for instrumental events), epicentral location, associated fault system, eruption linkage (×), and bibliographic sources. References: Guidoboni et al. (2014)1; Guidoboni et al. (2019)2; Azzaro and D'Amico (2019)3; Rovida et al. (2022)4. *Asterisk (*) indicates macroseismic magnitudes.*

N	Year CE	I0 MCS	M	distance from SVP (km)	Fault	Eruption	Ref
1	251					X	1
2	1818	9.5	6.2*	2.6			2
3	1848	7/8	5.0*	6.4			2
4	1855	7/8	4.0*	15.6	Moscarello		2
5	1865	9	4.9*	13.4	Moscarello	X	2,3
6	1879	8/9	4.6*	10.8	S. Venerina		2,3
7	1889	7/−8	4.0*	7.1	S. Tecla		2,3
8	1894	8/9	4.6*	9.3	Fiandaca		2,3
9	1907	9/10	4.0*	5.8	Fiandaca		3
10	1911	8/9	4.6*	12.8	Moscarello	X	2,3
11	1914	9/10	5.2*	8.4	S. Tecla		2,3
12	1920	7/8	4.0*	14.7	S. Leonardello		3
13	1952	7/8	4.0*	9	S. Tecla		3
14	1971	8	4.3	14.6	Moscarello		3
15	1984	8	4.4	9.6	Fiandaca		3
16	2002	8	4.5	10	S. Venerina	X	3,4
17	2018	8	4.8	7.5	Fiandaca	X	3,4

2.3. Seismicity and fault-magma interactions

Seismicity at Mount Etna is concentrated beneath the summit and along the southern and eastern flanks, where active faulting interacts with shallow magmatic intrusions (Giampiccolo et al., 2020, 2024; Alparone et al., 2020). In contrast, the northwestern flank shows deeper and more scattered events, typically below 15–20 km (Azzaro and D'Amico, 2019). The southeastern flank—particularly near Santa Venera al Pozzo—has experienced several damaging earthquakes, as evidenced by both historical accounts and archaeoseismological evidence (Guidoboni et al., 2014, 2019; Bottari et al., 2020). Although earthquake focal mechanisms are not always available, the spatial overlap between fault-related seismicity, eruptive fissures and hydrothermal vents highlights the existence of a mechanically coupled system linking tectonic deformation, magmatic intrusion, and fluid migration.

Recent instrumental records (1981–2024) show that seismicity clusters within the Timpe Fault System (TFS), particularly along the Fiandaca Fault (FF), and the Aci Catena–Aci Platani Faults (ACF–APF), which accommodate part of the volcano's flank spreading (Azzaro et al., 2012; Tringali et al., 2022). Focal depth distribution indicates that most events occur within the upper 5–6 km, consistent with the brittle response of the volcanic pile to magmatic pressure and gravitational loading.

Seismic swarms often precede or accompany eruptive episodes, confirming the tight coupling between fault motion and dike intrusion (Bevilacqua et al., 2022; Proietti et al., 2024). During the 2018 eruption, a segment of the Fiandaca Fault- long recognized as active - produced surface ruptures and ground deformation consistent with dike propagation from the summit toward the lower southeast flank (Aloisi et al., 2009).

This mechanism exemplifies how magma-driven fault slip contributes to the long-term instability of the flank and controls the localization of eruptive fissures and thermal springs. From a historical perspective, the recurrent seismicity affecting the Acireale–Aci Catena–Santa Venera corridor reflects the persistent reactivation of the same structural lineaments observed today.

These fault segments define preferential pathways for both magmatic ascent and hydrothermal circulation, forming the geological backbone that sustained long-term human settlement in this area. The

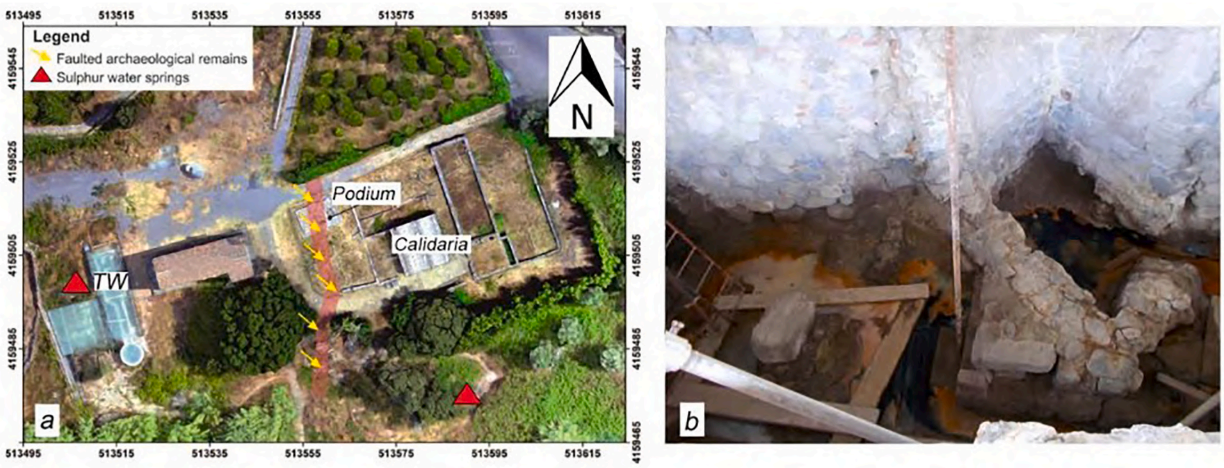

Fig. 3. Sulphur spring and archaeological evidence of faulting at Santa Venera al Pozzo (SVP). (a) Digital Surface Model (DSM) of the archaeological site showing the layout of the bath complex and associated structures. Yellow arrows indicate faulted archaeological remains (Bottari et al., 2018); red triangles mark active sulphur-water springs. Key architectural elements, including the *calidaria* and the *podium*, are labelled. TW denotes the most recent thermal-water spring, shown in panel (b). (b) Interior view of the sulphur spring emerging within the bath complex. The water maintains a stable temperature of approximately 22 °C. Sudden changes in colour, likely due to oxidation–reduction reactions, were historically interpreted as divine omens (photograph by S. Amari). (For interpretation of the references to colour in this figure legend, the reader is referred to the web version of this article.)

archaeological evidence of damage and reconstruction phases at SVP supports this view, suggesting that local communities repeatedly adapted to fault-related earthquakes while exploiting the geothermal resources associated with the same structures.

2.4. Volcano-tectonic coupling and seismic hazard at SVP

Building upon the structural and seismological framework discussed above, this section examines how volcano–tectonic interactions shape seismic hazard in the SVP area. The integration of instrumental, historical, and archaeological data provides a unique opportunity to reconstruct the impact of earthquakes over millennia.

A comprehensive seismic record (Table 1) reveals a recurrent association between tectonic faulting and volcanic activity along Mount Etna's southeastern flank. Several moderate to strong earthquakes—some coinciding with eruptive phases—have affected the region in the last two millennia (Guidoboni et al., 2014; Bottari et al., 2018). Among the most damaging were the 1818 CE (Mw 6.2) and 1848 CE (Mw 5.5) events, both responsible for widespread structural damage and ground fracturing (Azzaro, 2004; Guidoboni et al., 2019; Rovida et al., 2022). In more recent times, the 2002 Santa Venerina and 2018 Fleri earthquakes (Mw 4.5–4.8, depth < 3 km) have caused renewed concern for the safety of built heritage and local infrastructure (Palano et al., 2009; Branca and Abate, 2019; Alparone et al., 2020; Tringali et al., 2022).

This spatio-temporal clustering of seismic and eruptive activity supports the concept of volcano-tectonic coupling, whereby magmatic intrusions and fault movements mutually reinforce one another. Archaeological evidence from SVP, notably the 251 CE damage horizon, interpreted as coeval with both volcanic and seismic activity, emphasizes the long-term persistence of this interaction (Bottari et al., 2020). Creeping faults, such as the Fiandaca and Aci Catena faults (FF and ACF; Fig. 2b), further complicate the seismic scenario. While aseismic creep can release stress gradually and lower the likelihood of large ruptures along certain segments, it may also transfer strain to adjacent locked faults, thereby sustaining seismic hazard in unpredictable ways (Azzaro et al., 2000).

Understanding these interactions is essential to anticipate future risk scenarios and to design adaptive strategies for land-use, heritage-preservation, and community resilience in this tectonically active area. As summarized in Table 1, the historical and instrumental record reveals recurrent moderate-to-strong earthquakes spatially associated with the Timpe, Fiandaca, and Aci Catena faults, sometimes coinciding with eruptive episodes.

3. Geological favourability for human presence on Mount Etna

3.1. Thermal springs on the volcano: infrastructure, symbolism, and continuity

Thermal springs have played a pivotal role in the history of human settlement on Mount Etna since prehistoric times. Among the most prominent examples are the Salinelle near Paternò and SVP, both of which offer well-documented records of long-standing human use of geothermal waters (Branca et al., 2021). These hydrothermal systems ensured a reliable, year- round water supply of geothermal water that sustained agriculture, craftsmanship, and ritual practices in an otherwise hazardous volcanic environment.

The connection between hydrothermal activity and human culture is clearly visible in the archaeological record. At Paternò, Roman thermal baths from the 1st– 2nd centuries CE were preserved beneath mudflow deposits, providing early material evidence of ritual and therapeutic use (Cavallaro, 2021). These mud deposits formed from long-standing and still ongoing emission of multiphase fluids, consisting of a muddy liquid phase and a separate gas phase, from hydrothermal vents and mud volcanoes. The liquid phase originates from the interaction between warm, hypersaline water—originally a geothermal brine formed from the condensation of deep-seated, high-enthalpy magmatic fluids—and local clays belonging to the rock cover overlying the hydrothermal reservoir (Chiodini et al., 1996a, 1996b; Chicco et al., 2020). Such fluids reach the surface along tectonic structures with a main *E*-W direction, related with active tectonism that still affects Pleistocene sediments of Mount Etna's basement (Branca et al., 2011).

On Etna's southeastern flank, SVP stands out for its exceptional cultural continuity, preserving both Greek and Roman architectural elements, including a thermal complex with vaulted *calidaria* and a monumental *podium*—markers of successive phases of construction, adaptation and reuse (Branciforti, 2006; Fig. 3a). Strategically located along the ancient Pompeian Road connecting Messina and Catania, SVP likely served as a *statio* (a Roman waystation) and a ritual healing site, highlighting its dual role as a logistical and symbolic role (Amari, 2006; Brancato and Tortorici, 2021).

Table 2
Chemical composition of Santa Venera al Pozzo (SVP) spring waters (1978–2024). Mean concentrations (meq/L) of major cations—sodium (Na^+), potassium (K^+), calcium (Ca^{2+}), and magnesium (Mg^{2+})—and anions—chloride (Cl^-), sulfate (SO_4^{2-}), and bicarbonate (HCO_3^-)—together with physicochemical parameters obtained from geochemical analyses conducted between 1978 and 2024. TDS = total dissolved solids; pH = measure of acidity or alkalinity; Eh = redox potential, indicating the oxidizing or reducing conditions of the water.

	Temp.	pH	Eh	Na^+	K^+	Mg^{2+}	Ca^{2+}	HCO_3^-	Cl^-	NO_3^-	SO_4^{2-}	TDS
	°C		mV	meq/L	meq/L	meq/L	meq/L	meq/L	meq/L	meq/L	meq/L	mg/L
Mean	22.5	7.21	−228.4	87.8	1.4	14.1	5.8	12.2	93.3	4.7	3.9	7180.7
Standard error	0.1	0.03	42.6	6.5	0.1	1.3	0.8	1.0	6.9	2.9	0.7	71.0
Median	22.5	7.19	−280.0	96.4	1.4	16.3	4.5	13.9	102.7	0.3	2.9	7172.1
Mode	22.5	7.23	n.d.	n.d.	1.4	n.d.	n.d.	13.1	106.3	0.3	n.d.	n.d.
Standard deviation	0.3	0.13	153.5	26.9	0.5	5.4	3.2	4.1	28.6	10.3	2.7	245.8
Kurtosis	4.6	1.71	−1.6	5.7	2.8	1.3	5.5	4.6	5.5	3.2	2.1	−1.1
Skewness	−1.9	0.23	0.5	−2.6	−0.1	−1.6	2.2	−2.4	−2.5	2.2	1.6	0.1
Interval	1.2	0.57	398.0	98.2	2.5	18.6	12.5	13.4	104.0	27.9	9.9	769.3
Min.	21.6	6.93	−396.0	7.8	0.2	1.0	3.4	1.5	8.5	0.0	1.1	6786.4
Max.	22.8	7.50	2.0	106.0	2.7	19.6	15.9	14.9	112.5	27.9	11.0	7555.7

Data from Brusca et al. (2001); Minissale et al. (2019) and D'Alessandro (written communication).

No other hydrothermal site on Mount Etna exhibits such a well-documented sequence of architectural reuse, ritual significance, and settlement continuity. In this regard, SVP represents a unique case study for understanding how geothermal resources contributed to cultural resilience and the persistence of human presence in geodynamically active landscapes.

Excavations conducted in 2014 uncovered a mineral-rich thermal spring believed to correspond to the myth of Acis and Galatea as described in *Ovid's Metamorphoses*. The vivid account—"a dark red blood flowed, then it grew pale and murky… then it cleared… Akis emerged"—suggests that ancient observers interpreted natural colour shifts in the water as divine manifestations (Amari, 2014).

Beyond their symbolic dimension, these hydrothermal systems were structurally controlled by fault networks that channeled deep fluid to the surface- a topic explored in the following section. This synthesis of natural observation and symbolic meaning shows how ancient societies not only coexisted with volcanic processes but also incorporated them into their worldview, turning potential hazards into enduring elements of cultural identity. Further archaeological investigations revealed a large Roman villa in the northern sector of SVP, later repurposed as a ceramic production workshop between the early 4th and mid-5th century CE (Brancato and Tortorici, 2021). In contrast, the adjacent thermal complex underwent monumental reconstruction during the same period and was subsequently reused in the Medieval era as a *hospitalis*, highlighting the site's remarkable capacity for functional transformation across centuries (Amari, 2008; Brancato and Tortorici, 2021).

3.2. Reading the hot waters: geochemical stability and cultural significance of SVP springs

Although several hydrothermal sites occur on Mount Etna's flanks and summit area, SVP and the Salinelle stand out as notable outliers. At the Salinelle, mud-rich fluids with high salinity emerge at ~50 °C and are interpreted as the result of a shallow, confined system with strong magmatic gas input (Chiodini et al., 1996a, 1996b; Chicco et al., 2020). In contrast, SVP springs discharge clear, bicarbonate–sulfate waters at ~22 °C, with lower salinity and geochemical signatures indicative of a more mature, stable and deeply sourced geothermal system (Brusca et al., 2001; Minissale et al., 2019).

Chemical analyses of SVP waters — initiated in the early 19th century CE (Ferrara, 1811; De Gaetani, 1839; Marieni, 1870; Silvestri, 1873) — reveal that major ion concentrations have remained remarkably consistent over the past two centuries, underscoring the long-term resilience of the hydrothermal reservoir. Contemporary monitoring confirms this overall stability, though transient anomalies in redox-potential (Eh) and Na^+/Cl^- ratios have occasionally been observed (Table 2), likely reflecting episodic perturbations in gas–water equilibrium or deep fluid input.

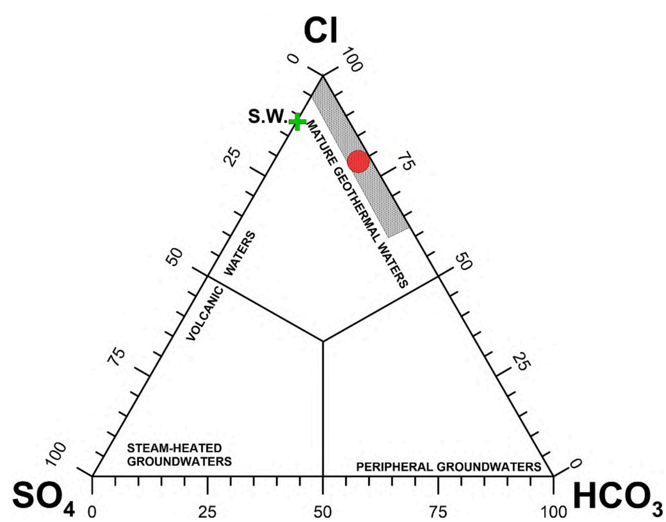

Fig. 4. Ternary diagram of major anion concentrations in SVP spring waters (1978–2024). The Cl^-–SO_4^{2-}–HCO_3^- classification diagram, based on water samples collected between 1978 and 2024, shows that compositions fall within the field typical of mature geothermal waters, as indicated by the median ionic ratios (red-filled circle). The green cross indicates the average composition of sea water (S.W.). Data from Brusca et al. (2001), Minissale et al. (2019) and D'Alessandro (written communication). (For interpretation of the references to colour in this figure legend, the reader is referred to the web version of this article.)

Such subtle variations may become visible: sulfide-rich waters, when oxidized at the surface, can shift in colour — from red to black or milky white. Far from being mere curiosities, these phenomena were historically perceived as divine manifestations, a belief deeply rooted in local myths and rituals (Amari, 2014; Fig. 3b).

Geochemically, SVP waters display characteristics of mature geothermal fluids, as shown in the classic Cl^-–SO_4^{2-}–HCO_3^- ternary diagram (Fig. 4). They also plot within the pyrite stability domain on the Eh–pH plot for iron–sulfide species (Fig. 5), indicating reducing conditions and the presence of dissolved hydrogen sulfide (H_2S), consistent with field observations of sulfide-rich waters that darken or turn milky white upon oxidation.

Saturation indices calculated with PHREEQC, suggest that the SVP waters are near or above saturation with respect to calcite, dolomite, and aragonite (Table 3). This implies the strong possibility of mineral precipitation at or near the water emergency point, suggesting extensive interaction between groundwaters and carbonate-bearing formations at

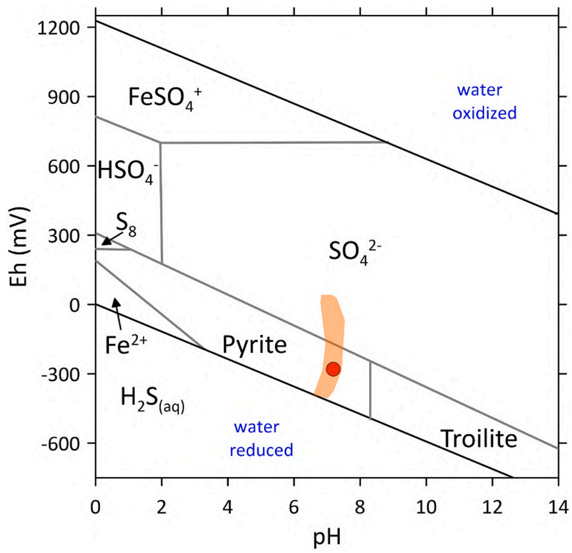

Fig. 5. Eh–pH diagram for SVP spring waters showing stability fields of iron species. Eh values of SVP waters display high variability (orange-shaded area), but most data plot within the pyrite stability field, as indicated by the median Eh and pH values (red circle). The diagram highlights the prevailing reducing conditions of SVP waters, consistent with pyrite precipitation. Modified after Garibello et al. (2022). (For interpretation of the references to colour in this figure legend, the reader is referred to the web version of this article.)

Table 3
Median values of saturation indices (SI) for the main mineral phases in SVP spring waters (1978–2024). The calculated SI values indicate equilibrium or slight oversaturation for calcite, dolomite, aragonite, quartz, chalcedony and talc, suggesting favorable conditions for the precipitation of these minerals under typical hydrothermal environments. Calculations performed using PHREEQC (Parkhurst and Appelo, 2013).

Mineral phase	S.I.
Anhydrite	−2.3
Aragonite	0.1
Calcite	0.2
Celestite	−1.3
Chalcedony	0.3
Chrysotile	−3.4
Dolomite	1.2
Gypsum	−1.9
Halite	−3.8
Quartz	0.7
Sepiolite	−1.9
SiO2(a)	−0.6
Strontianite	−0.4
Sylvite	−5.0
Talc	0.8

temperatures exceeding 50 °C. Occasional episodes of silica supersaturation, as shown by the data in Table 3, may also explain the transient white discoloration at the spring outlets.

Taken together, these features identify SVP as a rare convergence of geochemical stability and cultural continuity — where thermal waters have supported daily life, ritual meaning, and long-term human resilience in a volcanically active setting.

3.3. Seismology as a storyteller of the past

Seismological records offer a unique perspective for reconstructing the dynamics of Mount Etna's southeastern flank and its long-term interaction with human settlement. To provide a comprehensive picture of seismicity in the study area, we analyzed instrumental earthquake data collected between 1979 and 2024 by various seismological networks operating on Mount Etna (Figs. 2b, 5). The dataset includes events with $M \geq 2.5$ from multiple catalogs (Cosentino et al., 1982; Gresta and Patanè, 1987; Patanè et al., 2004; Distefano and Di Grazia, 2005; Alparone et al., 2020a, 2020b; Barberi et al., 2020; Alparone et al., 2022) and excludes microseismicity to ensure consistency despite changes in network sensitivity over time.

The southeastern flank of Mount Etna—where SVP is located—exhibits comparatively low seismicity. Since 1979 CE, only 38 crustal earthquakes (ML 2.5–4.5, local magnitude) have been recorded in this sector, accounting for approximately 1.5% of the total strain released across the volcano (Fig. 6). These events are concentrated in the northern part of the area and typically occur within the upper 13 km of the crust. The seismic record reveals alternating phases of quiescence and activity, with notable peaks in 1979–1987 CE and again in April 2023 CE, when a Mw 4.5 (moment magnitude) earthquake occurred offshore between Aci Castello and Aci Trezza at approximately 20 km depth.

It is well established that the persistent east–southeastward flank sliding of Mount Etna is accompanied by seismicity along the NNW–SSE Timpe Fault System (TFS), which intersects the SVP area (Azzaro et al., 2013; Urlaub et al., 2022), reflecting the combined effects of gravitational instability and recurrent magmatic intrusions (e.g., Acocella et al., 2003; Bonforte et al., 2013; Pezzo et al., 2020).

To further explore the relationship between magmatic processes and shallow seismicity, we analyzed earthquakes with hypocentral depths <5 km within the SVP area in relation to documented eruptive phases (Fig. 7). The analysis reveals pronounced increases in shallow crustal strain release during three key periods—1980–1986, 2001–2006, and 2018–2020 CE—each characterized by intense fissure eruptions and significant magma discharge Approximately 60% of shallow earthquakes occurred within these intervals, indicating strong temporal clustering and suggesting that magmatic intrusions into the upper crust act as a primary driver of localized seismicity.

When compared with the historical and archaeological record, the instrumental data reveal a consistent spatial correlation between fault zones, eruptive fissures, and damage horizons. This convergence underscores the importance of seismology as a bridge between present dynamics and past events, validating archaeoseismological interpretations such as the 251 CE destruction layer documented at SVP (Bottari et al., 2020). This dynamic encapsulates a fundamental duality: the same magmatic processes that elevate seismic hazard also sustain the hydrothermal systems that have long supported human settlement.

Understanding this balance is essential to interpreting how communities have historically adapted to—and coexisted with—the hazards and resources of an active volcanic environment.

3.4. Etna in motion: what geodesy reveals

Since the early 1990s, episodic and continuous GNSS measurements at Mount Etna have provided significant insights into the surface ground deformations affecting the volcano edifice. In particular, these observations have allowed the detection of: i) several volcano-wide inflation/deflation cycles (Palano et al., 2024 and reference therein), ii) shallow magmatic intrusions (Bonaccorso et al., 2002; Aloisi et al., 2003, 2009; Gambino et al., 2016), iii) a steady-state seaward movement of the eastern flank of the volcano (Palano et al., 2023), iv) a coseismic deformation pattern related to shallow earthquakes, v) viscoelastic deformation episodes (Palano et al., 2009; Pezzo et al., 2023), and vi) the occurrence of SSEs involving the basal sliding surface beneath the eastern flank of Mount Etna (Palano, 2016; Palano et al., 2022).

On the south-eastern flank, the long-term GNSS velocity field (Fig. 8) show a general SE- ward pattern with rates increasing from ~15 mm/yr,

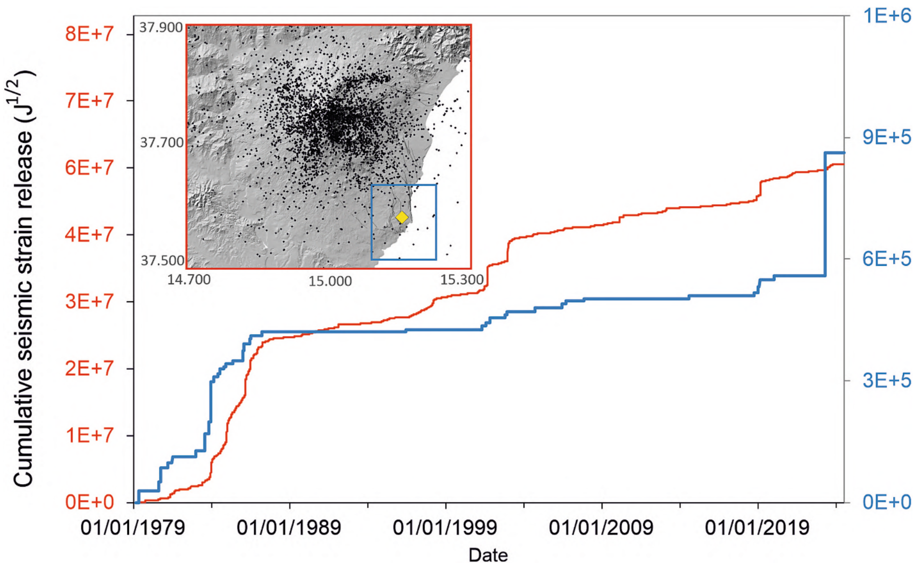

Fig. 6. Cumulative seismic strain release in the SVP sector (blue line) compared to the entire Mount Etna (red line). The SVP site is marked with the yellow diamond. Despite its volcano-tectonic complexity, the SVP area (which covers approximately 220 km^2) accounts for only about 1.5% of the total strain energy release from the entire volcano (which has a total size of approximately 2350 km^2). The seismic data come from the multiple seismological catalogs mentioned in the text. (For interpretation of the references to colour in this figure legend, the reader is referred to the web version of this article.)

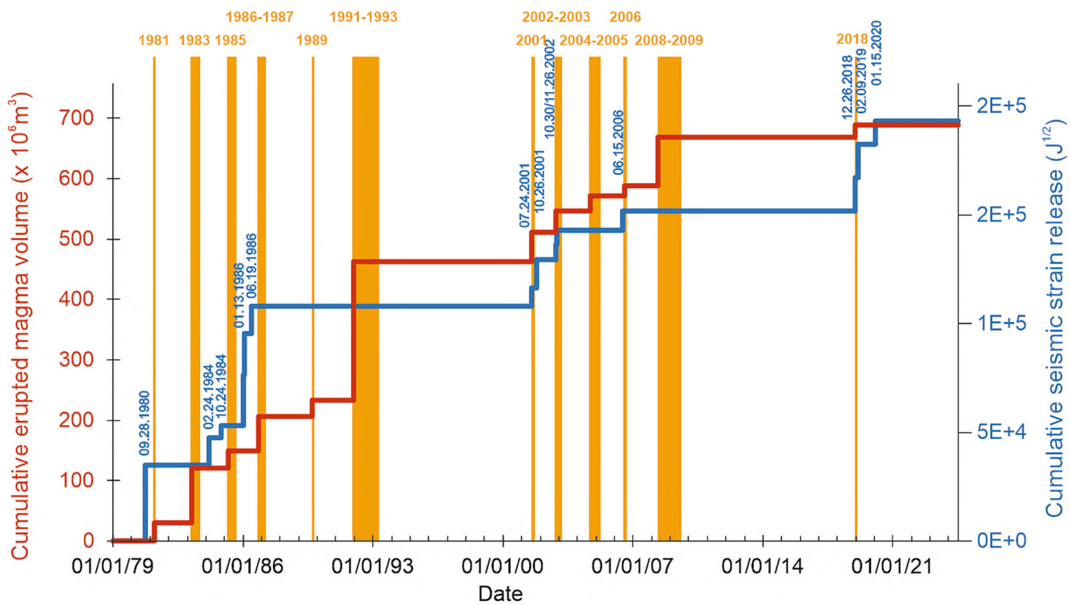

Fig. 7. Temporal correlation between eruptive episodes and shallow seismicity. Periods of increased seismic strain (<5 km depth) correspond to phases of high magma discharge (e.g., 1980–1986, 2001–2006, 2018–2020 CE). Magma volumes from Bonforte et al. (2013) and Pezzo et al. (2020).

on the intermediate eastern flank, up to ~40 mm/yr along the coastal belt, which occupies less than ~25% of the flank's surface, but accommodates the highest deformation rates. This acceleration is coupled with a general counterclockwise rotation of velocity vectors-from the ~N140°E direction, west of the Timpe Fault System, toward the ~N115°E direction, along the coastal belt-resulting in a crustal stretching (areal change and strain-axes in Fig. 8).

The sector west of the Aci Catena Fault (ACF) is characterized by an areal change rate of 1–3 microstrain/yr, whereas rates of 5–6 microstrain/yr occur along a narrow belt bounded by the Aci Catena and the sea (ACF; Fig. 8). This evidence indicates that most of the deformation is concentrated in this latter zone. Crustal stretching occurs along the *E*-W direction, orthogonal to the strike of most normal faults, suggesting that these structures - cutting the impermeable sedimentary basement - act as a preferential pathway for crustal fluid ascent. Indeed, geochemical measurements over the last five decades identify this same area as characterized by significant gas emissions, confirming the tight coupling between deformation, permeability, and hydrothermal activity.

4. Discussion: resilience, risk and rationality in settlement patterns

The long-term occupation of SVP illustrates how communities on Mount Etna actively responded to volcanic and seismic hazards by leveraging localized environmental advantages. Rather than passively enduring risk, inhabitants developed strategies that allowed them to settle—and persist—within a geodynamically/volcanically active landscape (Fig. 9).

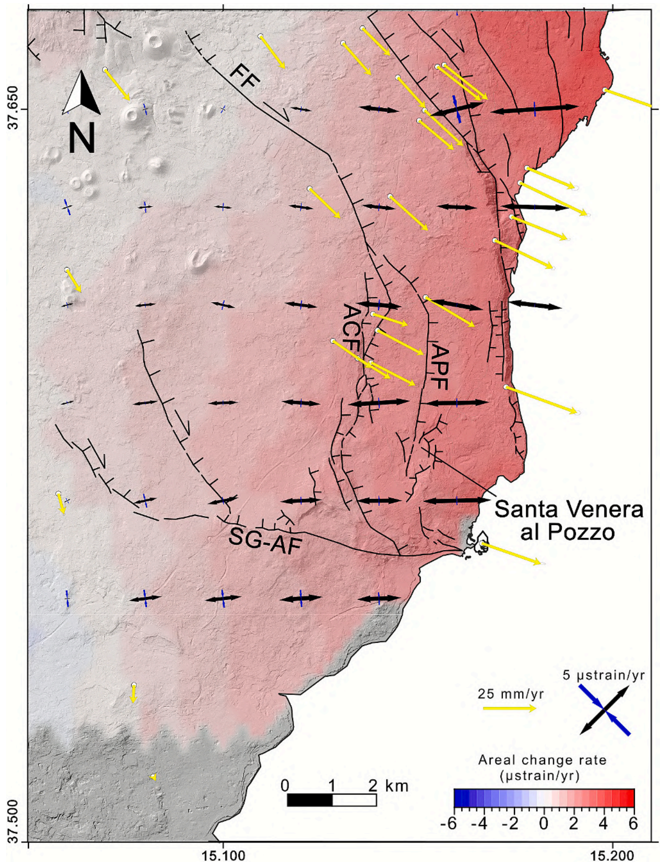

Fig. 8. GNSS-derived strain rate field and velocity field on the southeastern flank. Velocity field and areal strain rates indicate intense deformation in the sector around the Aci Platani Fault (APF). Fiandaca Fault (FF), Aci Catena Fault (ACF) and San Gregorio - Acitrezza Fault (SG-AF) are also highlighted. SE-ward motion and crustal stretching are evident. GNSS data from Palano et al., 2023); faults data from Azzaro et al. (2012).

SVP benefited from a unique combination of favorable conditions: fertile volcanic soils that sustained agriculture, geochemically stable thermal springs that ensured a reliable supply of potable and therapeutic water, and a location shielded from lava flows, lying outside Mount Etna's main rift zones and beyond the Valle del Bove collapse depression, as confirmed by geological records (Fig. 1a, b).

Although the site experienced damaging earthquakes- such as those in 251 CE and the mid-4th century CE, the recurrence of strong seismic events appears lower than in other parts of the volcano (Fig. 9). Local deformation was largely accommodated by aseismic creep along faults, which mitigated seismic risk while enhancing permeability for hydrothermal circulation (Figs. 8, 9).

The thermal springs of SVP played a central role in sustaining the settlement. Their chemical composition has remained remarkably stable over two centuries of observation (De Gaetani, 1839; Brusca et al., 2001), and their symbolic resonance is well documented in literary and archaeological sources. Changes in colour or clarity were often interpreted as divine manifestations (Amari, 2008), thus embedding the springs with both practical and spiritual value.

Strategically located near the Roman Pompeian Road and the ancient port of Capo Mulini, SVP also served as a logistical hub. Its function as a *statio*—and later as a production and bathing complex—demonstrates architectural adaptability and continuous reuse from the Roman (1st-4th century CE) through the Medieval period (9th–13th century CE; Branciforti, 2006; Amari, 2008).

This case study highlights how environmental knowledge, infrastructure resilience, and cultural meaning intersected to support long-term settlement. Rather than avoiding risk zones entirely, ancient communities engaged with their surroundings through a combination of spatial reasoning, symbolic frameworks, and practical adaptation. The SVP case illustrates that resilience in volcanic landscapes derives from the interaction of three factors: resource reliability, relative hazard stability, and cultural embeddedness. Settlement in hazardous environments is therefore not irrational, but adaptive. Beyond Etna, this triad provides a transferable model for interpreting long-term human persistence in other volcanic settings worldwide- from the Mediterranean to the Pacific- where hazard and resource are inseparably intertwined.

5. Conclusions: lessons from the past for volcanic futures

The case study of Santa Venera al Pozzo (SVP) exemplifies how ancient communities consciously balanced the opportunities and risks posed by a dynamic volcanic environment. As noted by Chester et al. (1985), many hazardous areas on active volcanoes worldwide have remained continuously occupied because inhabitants judged that the benefits outweighed the risks. On Mount Etna, this trade-off was expressed through the harnessing of geothermal resources, the strategic occupation of zones characterized by relatively low seismic release, and the development of cultural frameworks that rendered environmental uncertainty more manageable.

Our integrated approach, combining geological, geophysical, and archaeological evidence, demonstrates that settlement persistence at SVP was not accidental, but the result of informed decision-making grounded in long-term empirical observation and adaptive responses. Thermal springs provided economic and hygienic benefits while simultaneously fostering cultural continuity and symbolic meaning, reinforcing social cohesion despite recurrent natural disturbances. At the same time, they acted as sensitive indicators of the underlying geodynamic processes operating along Etna's southeastern flank.

These findings underscore that ancient resilience should not be interpreted as passive endurance, but rather as active engagement with complex geosystems. The SVP case proposes a broader conceptual model for understanding long-term habitability in geodynamically active landscapes and offers transferable insights for hazard planning, cultural heritage management, and sustainable development in volcanic regions worldwide, contributing to global Earth-system perspectives on human–environment interaction.

More broadly, these reflections invite consideration of how modern societies interact with active volcanic landscapes. The adaptive strategies observed at SVP suggest that resilience is not merely technological but also cultural and spatial. Understanding how past communities sustained ong-term coexistence with dynamic environments may therefore inform contemporary approaches to risk governance, land-use planning, and sustainable development.

CRediT authorship contribution statement

Carla Bottari: Writing – review & editing, Writing – original draft, Project administration, Methodology, Investigation, Data curation, Conceptualization. **Alessandro Luppino:** Visualization. **Salvatore Claudio Alparone:** Writing – review & editing, Validation, Investigation. **Francesca Forni:** Writing – review & editing. **Gianluca Groppelli:** Writing – review & editing, Validation, Investigation. **Mimmo Palano:** Writing – review & editing, Validation, Investigation. **Francesco Sortino:** Writing – review & editing, Validation, Investigation. **Salvatore Giammanco:** Writing – review & editing, Supervision, Methodology, Investigation, Conceptualization.

Declaration of competing interest

The authors declare that they have no known competing financial interests or personal relationships that could have appeared to influence

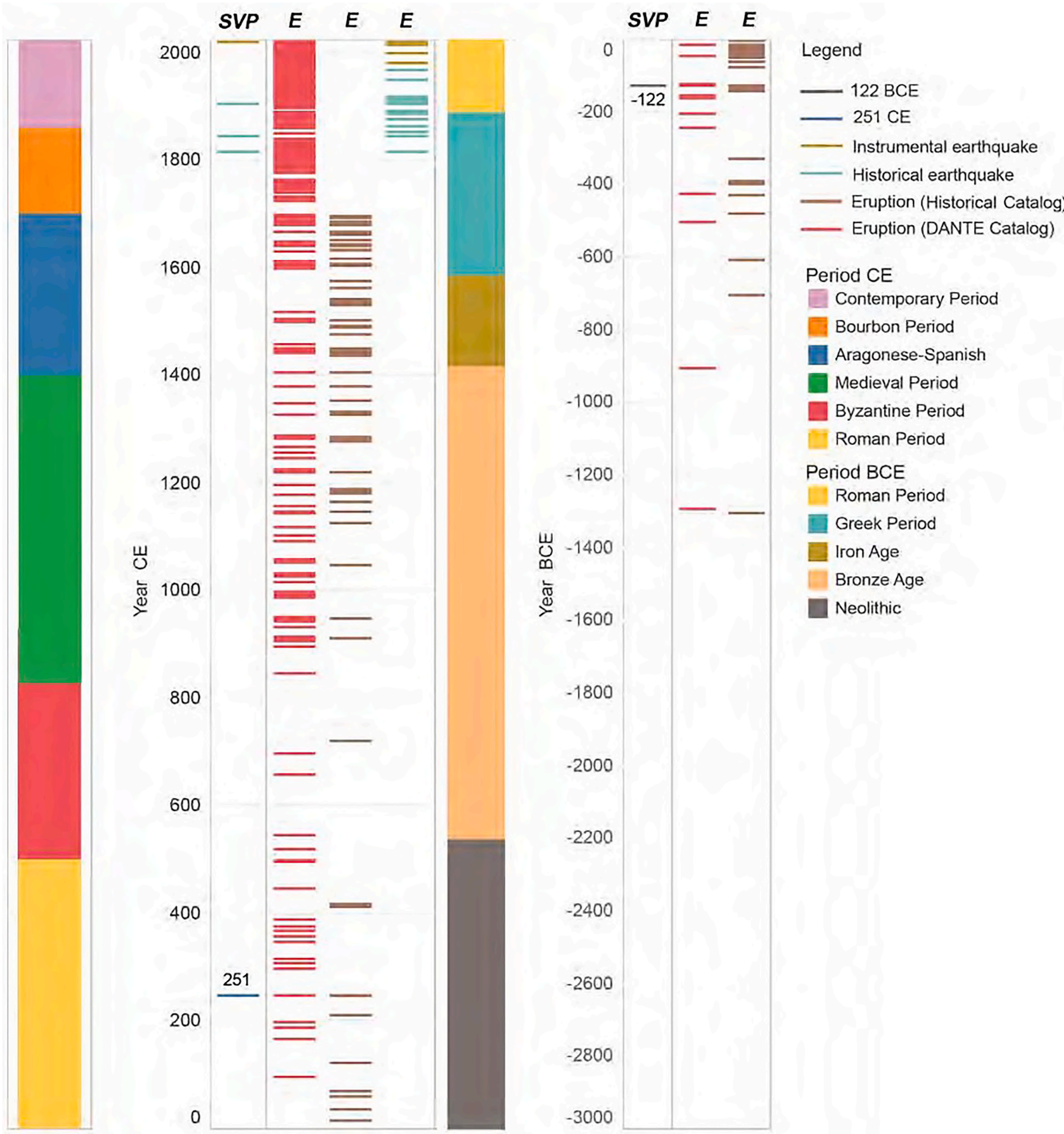

Fig. 9. Temporal correlation between volcanic and seismic events at Mount Etna and Acireale (SVP) from 3000 BCE to the present. The timeline illustrates eruptions from the DANTE catalog (Branca et al., 2025) and the historical catalog (Guidoboni et al., 2014), alongside instrumental earthquakes (light blue lines) and historical earthquakes (light brown lines). The 251 CE earthquake (blue line) represents a well-documented archaeoseismological event at SVP (Bottari et al., 2018), while the 122 BCE Plinian eruption (Coltelli et al., 1998; Branca and Del Carlo, 2004) (grey line) corresponds to one of the most explosive basaltic eruptions in Etna's history, marked by extensive tephra fallout and no associated lava flows. Cultural periods are indicated by colored vertical bands: CE periods on the left and BCE periods on the right.
Seismic and volcanic events are shown for both Mount Etna (E) and SVP, highlighting phases of increased geohazard activity that coincide with key settlement periods on the volcano's southeastern flank. (For interpretation of the references to colour in this figure legend, the reader is referred to the web version of this article.)

the work reported in this paper.

Acknowledgements

We thank Maria Costanza Lentini, Gioconda Lamagna, and the current director Giuseppe D'Urso, who have served as directors of the Archaeological Park of Catania and the Valley of the Aci, for authorizing and supporting the field and laboratory activities during the various phases of this research. We are grateful to Giulia Falco for her constant support throughout the work. We are also grateful to Susanna Amari for kindly providing the photograph used in Fig. 3.

We also thank the editor, Liviu Matenco, and the reviewers, Hripsime Gevorgyan and two anonymous for their insightful comments and constructive suggestions, which greatly improved the clarity and quality of this paper.

Data availability

All data supporting the findings of this study are available within the article.

Additional data (geochemical analyses, GNSS datasets, and field survey records) are archived at the INGV database and can be made available upon reasonable request to the corresponding author.

References

Acocella, V., Behncke, B., Neri, M., D'Amico, S., 2003. Link between major flank slip and eruptions at Mt. Etna (Italy). Geophys. Res. Lett. 30, 2286. https://doi.org/10.1029/2003GL018642.

Aloisi, M., Bonaccorso, A., Gambino, S., Mattia, M., Puglisi, G., 2003. Etna eruption imaged from continuous tilt and GPS data. Geophys. Res. Lett. 30 (23), 2214. https://doi.org/10.1029/2003GL018896.

Aloisi, M., Bonaccorso, A., Cannavò, F., Gambino, S., Mattia, M., Puglisi, G., Boschi, E., 2009. A new dike intrusion style for the Mount Etna May 2008 eruption modelled through continuous tilt and GPS data. Terra Nova 21 (4), 316–321. https://doi.org/10.1111/j.1365-3121.2009.00889.x.

Alparone, S., Barberi, G., Giampiccolo, E., Maiolino, V., Mostaccio, A., Musumeci, C., 2020. Seismological constraints on the 2018 Mt. Etna (Italy) flank eruption and implications for the flank dynamics of the volcano. Terra Nova 32, 334–344. https://doi.org/10.1111/ter.12463.

Alparone, S.C., Barberi, G., Di Grazia, G., Giampiccolo, E., Maiolino, V., Mostaccio, A., Musumeci, C., Scaltrito, A., Ursino, A., 2020a. Mt. Etna Seismic Catalog, 2011–2013 (Version 1) [Dataset]. INGV Publication, Rome, Italy. https://doi.org/10.13127/etnasc/etnarsc2020.

Alparone, S.C., Barberi, G., Di Grazia, G., Giampiccolo, E., Maiolino, V., Mostaccio, A., Musumeci, C., Scaltrito, A., Tuvè, T., Ursino, A., 2020b. Mt. Etna Seismic Catalog, 2014–2016 (Version 1) [Dataset]. INGV Publication, Rome, Italy. https://doi.org/10.13127/etnasc/2014_2016.

Alparone, S., Barberi, G., Di Grazia, G., Giampiccolo, E., Maiolino, V., Mostaccio, A., Musumeci, C., Scaltrito, A., Tuvè, T., Ursino, A., 2022. Mt. Etna Seismic Catalog, 2017–2019 (EtnaSC_2017_2019) (Version 1) [Dataset]. INGV Publication, Rome, Italy. https://doi.org/10.13127/etnasc/2017_2019.

Amari, S., 2006. I materiali in esposizione nell'Antiquarium – sale I–II–III. In: Branciforti, M.G. (Ed.), L'area archeologica di Santa Venera al Pozzo – Acium. Antiquarium, Palermo, pp. 105–183.

Amari, S., 2008. A late Roman amphorae production in Eastern Sicily. In: Menozzi, O., Di Marzio, M.L., Fossataro, D. (Eds.), SOMA 2005. Proceedings of the IX Symposium on Mediterranean Archaeology, BAR Int. Ser. 1739, pp. 473–479.

Amari, S., 2014. Observations on the late Roman coarse wares production from the factory of Acium in Sicily (Italy). BAR Int. Ser. 2616 (1), 225–234.

Apuani, T., Corazzato, C., Merri, A., Tibaldi, A., 2013. Understanding Etna flank instability through numerical models. J. Volcanol. Geotherm. Res. 251, 112–126. https://doi.org/10.1016/j.jvolgeores.2012.06.015.

Azzaro, R., 2004. Seismicity and active tectonics in the Etna region: Constraints for a seismotectonic model. Geophys. Monogr. Ser. 143, 205–220. https://doi.org/10.1029/143GM13.

Azzaro, R., D'Amico, S., 2019. Catalogo Macrosismico dei Terremoti Etnei (CMTE) [Dataset]. INGV Publication, Rome, Italy. https://doi.org/10.13127/cmte.

Azzaro, R., Barbano, M.S., D'Amico, S., Mostaccio, A., 2000. Tectonic and volcanic deformation at Mt. Etna: constraints from geodetic and seismic data. J. Geodyn. 29 (1–2), 187–210. https://doi.org/10.1016/S0264-3707(99)00049-1.

Azzaro, R., Branca, S., Gwinner, K., Coltelli, M., 2012. The volcano-tectonic map of Etna volcano, 1:100,000 scale: an integrated approach based on a morphotectonic analysis from high-resolution DEM constrained by geologic, active faulting and seismotectonic data. Ital. J. Geosci. 131, 153–170. https://doi.org/10.3301/IJG.2011.29.

Azzaro, R., Bonforte, A., Branca, S., Guglielmino, F., 2013. Geometry and kinematics of the fault systems controlling the unstable flank of Etna volcano (Sicily). J. Volcanol. Geotherm. Res. 160, 210–222. https://doi.org/10.1016/j.jvolgeores.2012.10.001.

Barberi, G., Di Grazia, G., Ferrari, F., Giampiccolo, E., Maiolino, V., Mostaccio, A., et al., 2020. Mt. Etna Revised Seismic Catalog 2020 (EtnaRSC2020) (Version 1) [Dataset]. INGV Publication, Rome, Italy. https://doi.org/10.13127/etnasc/etnarsc2020.

Barclay, J., Few, R., Armijos, M.T., Phillips, J.C., Pyle, D.M., Hicks, A., Brown, S.K., Robertson, R.E.A., 2019. Livelihoods, wellbeing and the risk to life during volcanic eruptions. Front. Earth Sci. 7, 205. https://doi.org/10.3389/feart.2019.00205.

Barsotti, S., Andronico, D., Neri, A., Del Carlo, P., Baxter, P.J., Aspinall, W.P., Hincks, T., 2010. Quantitative assessment of volcanic ash hazards for health and infrastructure at Mt. Etna (Italy) by numerical simulation. J. Volcanol. Geotherm. Res. 192 (1–2), 85–96. https://doi.org/10.1016/j.jvolgeores.2010.02.011.

Berger, G.W., 2006. The benefits of volcanic soils in ancient agriculture. Quat. Sci. Rev. 25, 215–229. https://doi.org/10.1016/j.quascirev.2005.01.006.

Bevilacqua, A., Azzaro, R., Branca, S., D'Amico, S., Flandoli, F., Neri, A., 2022. Quantifying the statistical relationships between flank eruptions and major earthquakes at Mt. Etna volcano (Italy). J. Geophys. Res. Solid Earth 127, e2022JB024145. https://doi.org/10.1029/2022JB024145.

Biscari, I.P., 1781. Viaggio per tutte le antichità della Sicilia. Stamperia Simoniana, Napoli.

Bonaccorso, A., Calvari, S., 2013. Major effusive eruptions and recent lava fountains: Balance between expected and erupted magma volumes at Etna volcano. Geophys. Res. Lett. 40, 6069–6073. https://doi.org/10.1002/2013GL058291.

Bonaccorso, A., Aloisi, M., Mattia, M., 2002. Dike emplacement forerunning the Etna July 2001 eruption modeled through continuous tilt and GPS data. Geophys. Res. Lett. 29 (13), 1624. https://doi.org/10.1029/2001GL014397.

Bonforte, A., Guglielmino, F., Puglisi, G., 2013. Interaction between magma intrusion and flank dynamics at Mt. Etna in 2008, imaged by integrated dense GPS and DInSAR data. Geochem. Geophys. Geosyst. 14, 2818–2835. https://doi.org/10.1002/ggge.20190.

Bonforte, A., Guglielmino, F., Puglisi, G., 2019. Large dyke intrusion and small eruption: The December 24, 2018 Mt. Etna eruption imaged by Sentinel-1 data. Terra Nova 31 (4), 405–412. https://doi.org/10.1111/ter.12403.

Borgia, A., Ferrari, L., Pasquaré, G., 1992. Importance of gravitational spreading in the tectonic and volcanic evolution of Mount Etna. Nature 357, 231–235. https://doi.org/10.1038/357231a0.

Bottari, C., Martorana, R., Scudero, S., Capizzi, P., Cavallaro, D., Pisciotta, A., D'Alessandro, A., Coltelli, M., Lodato, L., 2018. Coseismic damage at an archaeological site in Sicily, Italy: evidence of Roman Age earthquake surface faulting. Surv. Geophys. 39, 1263–1284. https://doi.org/10.1007/s10712-018-9482-2.

Bottari, C., Giammanco, S., Cavallaro, D., Sortino, F., Scudero, S., Amari, S., Bonfanti, P., Daolio, M., Groppelli, G., 2020. How to reveal unknown hidden faults and historical earthquake damage applying multidisciplinary methods in archaeological sites: the case of mid-third century CE Mt. Etna earthquake (Eastern Sicily, Italy). Tectonophysics 790, 228544. https://doi.org/10.1016/j.tecto.2020.228544.

Bousquet, J.C., Lanzafame, G., 2004. The tectonics and geodynamics of Mt. Etna: Synthesis and interpretation of geological and geophysical data. In: Bonaccorso, A., Calvari, S., Coltelli, M., Del Negro, C., Falsaperla, S. (Eds.), Mt. Etna: Volcano Laboratory, Geophys. Monogr. Ser. 143. https://doi.org/10.1029/143GM03. Ch. 3.

Bousquet, J.C., Lanzafame, G., Paquin, C., 1988. Tectonic stresses and volcanism: in-situ stress measurements and neotectonic investigations in the Etna area (Italy). Tectonophysics 149 (1–2), 219–231. https://doi.org/10.1016/0040-1951(88)90174-0.

Branca, S., Abate, D., 2019. Current knowledge of Etna's flank eruptions (Italy) occurring over the past 2500 years. J. Volcanol. Geotherm. Res. 385, 159–178. https://doi.org/10.1016/j.jvolgeores.2017.11.004.

Branca, S., Del Carlo, P., 2004. Eruptions of Mt. Etna during the past 3200 years: a revised compilation integrating the historical and stratigraphic records. Geophys. Monogr. Ser. 143, 1–28. https://doi.org/10.1029/143GM02.

Branca, S., Coltelli, M., Groppelli, G., Lentini, F., 2011. Geological map of Etna volcano, 1:50,000 scale. Ital. J. Geosci. 130, 265–291. https://doi.org/10.3301/IJG.2011.15.

Branca, S., Condomines, M., Tanguy, J.-C., 2015. Flank eruptions of Mt Etna during the Greek, Roman and early medieval periods: new data from 226Ra–230Th dating and archaeomagnetism. J. Volcanol. Geotherm. Res. 304, 265–271. https://doi.org/10.1016/j.jvolgeores.2015.09.002.

Branca, S., De Beni, E., Chester, D., Duncan, A., Lotteri, A., 2017. The 1928 eruption of Mount Etna (Italy): reconstructing lava flow evolution and the destruction and recovery of the town of Mascali. J. Volcanol. Geotherm. Res. 335, 54–70. https://doi.org/10.1016/j.jvolgeores.2017.02.002.

Branca, S., Privitera, F., Palio, O., Turco, M., 2021. Prehistoric human presence on Mount Etna (Sicily), in relation to the geological evolution. Ann. Geophys. 64 (5), VO542. https://doi.org/10.4401/ag-8667.

Branca, S., Del Carlo, P., Behncke, B., Bonfanti, P., 2025. Database of Etna's Historical Eruptions (DANTE) (Version 1) [Dataset]. INGV Publication, Rome, Italy. https://doi.org/10.13127/etna/dante.

Brancato, R., Tortorici, E., 2021. Carta Archeologica del territorio delle Aci. Edizioni Quasar, Roma.

Branciforti, M.G., 2006. L'area archeologica di Santa Venera al Pozzo – Acium. Antiquarium, Palermo.

Brusca, L., Aiuppa, A., D'Alessandro, W., Parello, F., Allard, P., Agnès, M., 2001. Geochemical mapping of magmatic gas–water–rock interactions in the aquifer of Mount Etna volcano. J. Volcanol. Geotherm. Res. 108, 199–218. https://doi.org/10.1016/S0377-0273(00)00286-9.

Calderone, D., De Giorgi, G., 2024. Archaeology and geomorphology of an area: New interpretations of long-term settlement logics from Prehistory to the Byzantine period across the central-eastern slopes of the Etna volcano. Thiasos 13, 35–51.

Cavallaro, B., 2021. La collina di San Marco: dati preliminari sulle tegole. In: Centamore, C., Ursino, M. (Eds.), La Collina di San Marco a Paternò. Percorsi di turismo sostenibile (Atti del Convegno 2017). SiciliAntica, pp. 115–118.

Chester, D.K., Duncan, A.M., Guest, J.E., Kilburn, C.R.J., 1985. Mount Etna: The Anatomy of a Volcano. Chapman and Hall, London.

Chicco, J.M., Giammanco, S., Mandrone, G., Nicolosi, A., Olocco, L., 2020. The "Salinelle of Mt. Etna" geosite: thermo-physical and geochemical monitoring of hydrothermal fluids aimed at understanding both their geothermal potential and their possible correlations with Mt. Etna activity. In: Abstract Volume, 4a Conferenza A. Rittmann, Catania, 12–14 February 2020.

Chiodini, G., D'Alessandro, W., Parello, F., 1996a. Geochemistry of the gases and of the waters discharged by the mud volcanoes of Paternò, Mt. Etna (Italy). Bull. Volcanol. 58, 51–58. https://doi.org/10.1007/s004450050125.

Chiodini, G., Frondini, F., Raco, B., 1996b. Diffuse emission of CO_2 from the Fossa crater, Vulcano Island (Italy). Bull. Volcanol. 58, 41–50. https://doi.org/10.1007/s004450050124.

Cocina, O., Neri, G., Privitera, E., Spampinato, S., 1998. Seismogenic stress field beneath Mt. Etna (South Italy) and possible relationships with volcano-tectonic features.

J. Volcanol. Geotherm. Res. 83 (3–4), 335–348. https://doi.org/10.1016/S0377-0273(98)00026-2.
Coltelli, M., Del Carlo, P., Vezzoli, L., 1998. Discovery of a Plinian basaltic eruption of Roman age at Etna volcano, Italy. Geology 26 (12), 1095–1098. https://doi.org/10.1130/0091-7613(1998)026.
Cosentino, M., Lombardo, G., Patanè, G., Schick, R., Sharp, A.D.L., 1982. Seismological research on Mount Etna: state of the art and recent trends. Mem. Soc. Geol. It. 23, 159–205.
De Beni, E., Branca, S., Coltelli, M., Groppelli, G., 2011. 40Ar/39Ar isotopic dating of Etna volcanic succession. Ital. J. Geosci. 130 (3), 292–305. https://doi.org/10.3301/IJG.2011.14.
De Gaetani, G., 1839. Sopra l'acqua solforosa del pozzo di S. Venera. In: Atti Acc. Gioenia Ser. 1, XIV, Catania.
Del Carlo, P., Vezzoli, L., Coltelli, M., 2004. Last 100 ka tephrostratigraphic record of Mount Etna. In: Bonaccorso, A., Calvari, S., Coltelli, M., Negro, C.D., Falsaperla, S. (Eds.), Mt. Etna: Volcano Laboratory, Geophys. Monogr. Ser. 143. https://doi.org/10.1029/143gm06.
Distefano, G., Di Grazia, G., 2005. Database localizzazioni ipocentrali terremoti Etna dal 1977 al 2001 [dataset]. In: Progetto DPC–INGV V3, Convenzione INGV-DPC 2004–2006, Task 4–Deliverable 4.2.2.
Ferrara, A., 1811. Memoria sopra le acque della Sicilia: Loro natura, analisi, ed usi. Dennet J, London.
Firetto Carlino, M., Cavallaro, D., Coltelli, M., Cocchi, L., Zgur, F., Patanè, D., 2019. Time and space scattered volcanism of Mt. Etna driven by strike-slip tectonics. Sci. Rep. 9, 12125. https://doi.org/10.1038/s41598-019-48550-1.
Gambino, S., Cannata, A., Cannavò, F., La Spina, A., Palano, M., Sciotto, M., Spampinato, L., Barberi, G., 2016. The unusual 28 December 2014 dike-fed paroxysm at Mount Etna: timing and mechanism from a multidisciplinary perspective. J. Geophys. Res. Solid Earth 121, 2037–2054. https://doi.org/10.1002/2015JB012379.
Garibello, C.F., Simonov, A.N., Eldridge, D.S., Malherbe, F., Hocking, R.K., 2022. Redox properties of iron sulfides: Direct versus catalytic reduction and implications for catalyst design. ChemCatChem 14, e202200270. https://doi.org/10.1002/cctc.202200270.
Giampiccolo, E., Cocina, O., De Gori, P., Chiarabba, C., 2020. Dyke intrusion and stress-induced collapse of volcano flanks: the example of the 2018 Etna eruption. Sci. Rep. 10, 6373. https://doi.org/10.1038/s41598-020-63371-3.
Giampiccolo, E., Tuvè, T., Bianco, F., Del Pezzo, E., 2024. Depth and spatial variation of the shear wave attenuation field at Mt. Etna: new insights into the plumbing system structure. Pure Appl. Geophys. 181, 1–17. https://doi.org/10.1007/s00024-023-03400-0.
Gresta, S., Patanè, G., 1987. Review of seismological studies at Mount Etna. Pure Appl. Geophys. 125, 951–970. https://doi.org/10.1007/BF00879362.
Gross, F., Krastel, S., Geersen, J., Behrmann, J.H., Ridente, D., Chiocci, F.L., Bialas, J., Papenberg, C., Çukur, D., Urlaub, M., Micallef, A., 2016. The limits of seaward spreading and slope instability at the continental margin offshore Mt Etna, imaged by high-resolution 2D seismic data. Tectonophysics 667, 63–76. https://doi.org/10.1016/j.tecto.2015.11.011.
Guidoboni, E., Ciuccarelli, C., Mariotti, D., Comastri, A., Bianchi, M.G., 2014. L'Etna nella Storia. In: Catalogo delle eruzioni dall'antichità alla fine del XVII secolo. Bononia Univ. Press, Bologna.
Guidoboni, E., Ferrari, G., Tarabusi, G., Sgattoni, G., Comastri, A., Mariotti, D., Ciuccarelli, C., Bianchi, M.G., Valensise, G., 2019. CFTI5Med: the new release of the catalogue of strong earthquakes in Italy [dataset]. Sci. Data 6, 188. https://doi.org/10.1038/s41597-019-0091-9.
Gvirtzman, Z., Nur, A., 1999. The formation of Mount Etna as the consequence of slab rollback. Nature 401, 782–785. https://doi.org/10.1038/44555.
Harris, A., Steffke, A., Calvari, S., Spampinato, L., 2011. Thirty years of satellite-derived lava discharge rates at Etna: implications for steady volumetric output. J. Geophys. Res. Solid Earth 116, B08204. https://doi.org/10.1029/2011JB008237.
James, P.A., Robson, G.R., Harris, M.B., 2000. Volcanoes and human history: the impact of eruptions on past civilizations. Earth Sci. Rev. 51, 187–216. https://doi.org/10.1016/S0012-8252(00)00020-0.
Kelman, I., Mather, T.A., 2008. Living with volcanoes: the sustainable livelihoods approach for volcano-related opportunities. J. Volcanol. Geotherm. Res. 172 (3–4), 189–198. https://doi.org/10.1016/j.jvolgeores.2007.12.007.
Liotta, M., D'Alessandro, W., Arienzo, I., Longo, M., 2017. Tracing the circulation of groundwater in volcanic systems using the $^{87}Sr/^{86}Sr$ ratio: Application to Mt. Etna. J. Volcanol. Geotherm. Res. 331, 102–107. https://doi.org/10.1016/j.jvolgeores.2017.01.002.
Lundgren, P., Berardino, P., Coltelli, M., Fornaro, G., Lanari, R., Puglisi, G., Sansosti, E., Tesauro, M., 2003. Coupled magma chamber inflation and sector collapse slip observed with synthetic aperture radar interferometry on Mt. Etna volcano. J. Geophys. Res.: Solid Earth 108 (B5).
Marieni, L., 1870. Geografia medica dell'Italia – Acque minerali. F. Vallardi, Napoli.
Minissale, A., Donato, A., Procesi, M., Pizzino, L., Giammanco, S., 2019. Systematic review of geochemical data from thermal springs, gas vents and fumaroles of Southern Italy for geothermal favourability mapping. Earth Sci. Rev. 188, 514–535. https://doi.org/10.1016/j.earscirev.2018.09.008.
Neri, M., Acocella, V., Behncke, B., 2004. The role of the Pernicana Fault System in the spreading of Mt. Etna (Italy) during the 2002–2003 eruption. Bull. Volcanol. 66, 417–430. https://doi.org/10.1007/s00445-003-0322-x.
Palano, M., 2016. Slow slip events beneath Mount Etna's eastern flank: evidence fromong-term GNSS observations. J. Volcanol. Geotherm. Res. 324, 8–14. https://doi.org/10.1016/j.jvolgeores.2016.05.010.
Palano, M., Calcaterra, S., Gambino, P., Porfidia, B., Sparacino, F., 2023. GNSS-based long-term deformation at Mount Etna volcano (Italy). Res. Geophys. Sci. 14, 100056.
Palano, M., Gresta, S., Puglisi, G., 2009. Time-dependent deformation of the eastern flank of Mt. Etna: after-slip or viscoelastic relaxation? Tectonophysics 473 (3–4), 300–311. https://doi.org/10.1016/j.tecto.2009.02.047.
Palano, M., Sparacino, F., Gambino, P., D'Agostino, N., Calcaterra, S., 2022. Slow slipevents and flank instability at Mt. Etna volcano (Italy). Tectonophysics 836, 229414. https://doi.org/10.1016/j.tecto.2022.229414.
Palano, M., Calcaterra, S., Gambino, P., Porfidia, B., Sparacino, F., 2023. GNSS-based long-term deformation at Mount Etna volcano (Italy). Results Geophys. Sci. 14, 100056. https://doi.org/10.1016/j.ringps.2023.100056.
Palano, M., Pezzo, G., Chiarabba, C., 2024. Magma budget, plutonic growth and lateral spreading at Mt. Etna. Commun. Earth Environ. 5, 95. https://doi.org/10.1038/s43247- 024-01267-0.
Parkhurst, D.L., Appelo, C.A.J., 2013. Description of Input and Examples for PHREEQC Version 3—A Computer Program for Speciation, Batch-Reaction, One-Dimensional Transport, and Inverse Geochemical Calculations. U.S. Geological Survey Techniques and Methods book 6, chap. A43, 497 p.
Patanè, D., Cocina, O., Falsaperla, S., Privitera, E., Spampinato, S., 2004. Mt. Etna volcano: a seismological framework. In: Bonaccorso, A., Calvari, S., Coltelli, M., Del Negro, C., Falsaperla, S. (Eds.), Mt. Etna: Volcano Laboratory, Geophys. Monogr. Ser. 143, pp. 147–165. https://doi.org/10.1029/GM143.
Pezzo, G., Palano, M., Tolomei, C., De Gori, P., Calcaterra, S., Gambino, P., Chiarabba, C., 2020. Flank sliding: a valve and a sentinel for paroxysmal eruptions and magma ascent at Mount Etna, Italy. Geology 48, 1077–1082. https://doi.org/10.1130/G47656.1.
Pezzo, G., Palano, M., Beccaro, L., Tolomei, C., Albano, M., Atzori, S., Chiarabba, C., 2023. Coupling flank collapse and magma dynamics on stratovolcanoes: the Mt. Etna example from InSAR and GNSS observations. Remote Sens. 15, 847. https://doi.org/10.3390/rs15030847.
Prayoga, R.A., Wahyono, E., Solekhah, N., Nurul Hakim, F., Fatimah, S., Purbandini, L., Wibowo, D.P., Saparita, R., 2024. Resilience rising: redefining livelihood systems in disaster-prone rural communities. Progr. Disast. Sci. 24, 100391. https://doi.org/10.1016/j.pdisas.2024.100391.
Proietti, C., De Beni, E., Cantarero, M., 2024. One hundred lava flows of Mt. Etna, Italy: July 2019–December 2023 update. J. Maps 20, 1–13. https://doi.org/10.1080/17445647.2024.2380899.
Riede, F., Barnes, G., Elson, M.D., Oetelaar, G.A., Holmberg, K.G., Sheets, P., 2020. Prospects and pitfalls in integrating volcanology and archaeology: a review. J. Volcanol. Geotherm. Res. 401, 106977. https://doi.org/10.1016/j.jvolgeores.2020.106977.
Rovida, A., Locati, M., Camassi, R., Lolli, B., Gasperini, P., Antonucci, A., 2022. Italian Parametric Earthquake Catalogue (CPTI15), Version 4.0 [Dataset]. INGV Publication, Rome, Italy. https://doi.org/10.13127/cpti/cpti15.4.
Ruch, J., Pepe, S., Casu, F., Acocella, V., Neri, M., Solaro, G., Sansosti, E., 2012. How do volcanic rift zones relate to flank instability? Evidence from collapsing rifts at Etna. Geophysical rùèesearch letters 39 (20).
Sartorius von Waltershausen, W., 1859. Der Aetna. Vol. 2: Die Gesteine des Aetna. Verlag der Hahn'schen Hofbuchhandlung, Hannover.
Silvestri, O., 1873. Sulle sorgenti idrogassose solfuree dette di S. Venera al Pozzo allabase orientale dell'Etna. In: Atti Acc. Gioenia Ser. 3, VIII, Catania, p. 102.
Small, C., Naumann, T., 2001. The global distribution of human population and recent volcanism. Environ. Hazards 3, 93–109. https://doi.org/10.1016/S1464-2867(02)00002-5.
Solaro, G., Acocella, V., Pepe, S., Ruch, J., Neri, M., Sansosti, E., 2010. Anatomy of an unstable volcano from InSAR: Multiple processes affecting flank instability at Mt. Etna, 1994–2008. J. Geophys. Res.: Solid Earth 115 (B10).
Sortino, F., Giammanco, S., Bonfanti, P., Bottari, C., 2022. Stress-induced changes in hydrothermal gas discharges along active faults near Mt. Etna volcano (Sicily, Italy). Tectonophysics 836, 229388. https://doi.org/10.1016/j.tecto.2022.229388.
Tibaldi, A., Groppelli, G., 2002. Volcano-tectonic activity along structures of the unstable NE flank of Mt. Etna (Italy) and their possible origin. J. Volcanol. Geotherm. Res. 115, 277–302. https://doi.org/10.1016/S0377-0273(01)00305-5.
Tibaldi, A., Luppino, A., De Beni, E., Corti, N., Cantarero, M., Mariotto, F.P., Bonali, F.L., 2025. Effects of lateral dyke propagation and pre-existing fractures on shallow deformation: Data from the Etna 1947 eruption and analogue models. J. Volcanol. Geotherm. Res. 108349. https://doi.org/10.1016/j.jvolgeores.2025.108349.
Torrence, R., 2019. Social responses to volcanic eruptions: a review of key concepts. Quat. Int. 499, 258–265. https://doi.org/10.1016/j.quaint.2018.02.033.
Tringali, G., Bella, D., Livio, F., Ferrario, M.F., Groppelli, G., Blumetti, A.M., Manna, P.D., Vittori, E., Guerrieri, L., Porfido, S., Boso, D., Pettinato, R., Paradiso, G., Michetti, A. M., 2022. Fault rupture and aseismic creep accompanying the December 26, 2018, Mw 4.9 Fleri earthquake (Mt. Etna, Italy): factors affecting the surface faulting in a volcano-tectonic environment. Quat. Int. https://doi.org/10.1016/j.quaint.2021.12.019.
Tringali, G., Bella, D., Livio, F., Ferrario, M.F., Groppelli, G., Pettinato, R., Michetti, A.M., 2023. Aseismic creep and gravitational sliding on the lower eastern flank of Mt. Etna: insights from the 2002 and2022 fault rupture events between Santa Venerina and Santa Tecla. Tectonophysics 856, 229829. https://doi.org/10.1016/j.tecto.2023.229829.
Urlaub, M., Gross, F., Krastel, S., Geersen, J., 2022. The submarine boundaries of Mount Etna's unstable southeastern flank. Front. Earth Sci. 10, 810790. https://doi.org/10.3389/feart.2022.810790.
Vergara-Pinto, F., Marín, A., 2023. Stratigraphy of volcanic memory: Sociocultural dimensions of volcanic risk in the Southern Andes, Chile. J. Conting. Crisis Manag. 31 (4), 1018–1033. https://doi.org/10.1111/1468-5973.12474.